

Violet: Architecturally Exposed Orchestration, Movement, and Placement for Generalized Deep Learning

Michael Davies, Karthikeyan Sankaralingam
{davies, karu}@cs.wisc.edu

Abstract

Deep learning and hardware for it has garnered immense academic and industry interest in the past 5 years, with many novel proposals. However, the state-of-art remains NVIDIA’s TensorCore-based systems that provide top-of-line **performance** and **coverage** across a wide-spectrum of deep learning applications. In this paper, we first identify four key problems any new DL solution must solve: 1) Data orchestration, 2) Data movement, 3) Work placement and blending these to achieve 4) Coverage across different types of DL applications. With this as a guide, we propose Violet, a novel architecture with roots in multicore SIMD which balances the responsibilities for these four problems between the architecture, microarchitecture and software stack. Compared to the NVIDIA A100 GPU, we find Violet achieves geo-mean 2.4X/10.6X and 2.1X/9.5X performance/efficiency for inference and training across the MLPerf benchmark suite. We present detailed operator-level analysis of the MLPerf benchmark suite, extracting out key behaviors – with implications for architecture research beyond this paper, that underpin the speedup and efficiency. Overall, this paper motivates the importance of balance, that the break down of responsibilities must be thought through carefully in order to compete with incumbent architecture designs.

1. Introduction

Deep Learning (DL) is one of the hottest topics in computing today, and its need for compute is insatiable. To meet this need, many styles of accelerator architecture are being explored, including NVIDIA’s [36], AMD’s [8] and Biren’s [18] GEMM engines, Google’s TPU [24], dataflow and spatially programmed architectures like Xilinx Versal [51], Graphcore [32], SambaNova [49], Groq [15], Qualcomm’s AI-100 [16], and other proposals [42, 5, 47, 38]. There is also some delineation between training vs inference, and within that, support for particular types of DNNs (CNN, LSTM, GNNs etc.).

Successful DL accelerators are quantified by their *coverage* of DL applications, and *performance*, *energy efficiency*, and *dollar cost* of those applications. Through this lens, NVIDIA’s TensorCore-based GPUs continue to be the dominant DL acceleration platform – supporting nearly every existing DL application as well as setting nearly every record for performance on the standard MLPerf [39] benchmark suite. Meanwhile, most other industry and academic contenders only report inference results for Resnet50 or BERT – and even in these cases,

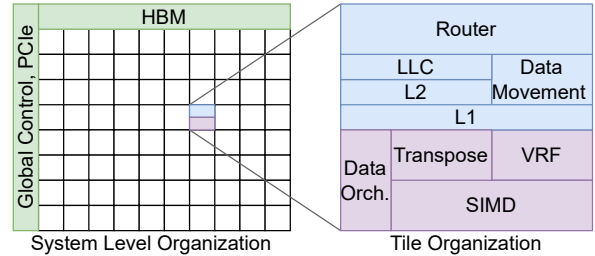


Figure 1: Overview of the Violet Architecture.

their performance is typically worse than NVIDIA. We term this apparent lack of performance and coverage from novel alternatives to GEMM acceleration, the *DL accelerator gap*.

To help explain the mechanisms underpinning the DL accelerator gap, we identify, for any new DL accelerator architecture, four primary problems which must be addressed: 1) **work placement** – how work for a given DL operation is divided and assigned to the architectural resources, 2) **data orchestration** – how data required for some portion of work is moved to the compute resource, 3) **data movement** – how the compute resource handles unpacking and processing the data to carry out its task, and 4) **coverage** – how the architecture and its software stack support generality and scalability across the domain of DL. We take the view that **balancing** the responsibilities for these problems between hardware, programmer, and software stack is key to bridging the DL accelerator gap and achieve this balance by exposing it to the architecture. We revisit these four problems throughout the paper to show how they are interrelated and how our design solves them.

Existing academic proposals for DL accelerators attempt to address these problems in a variety different ways but fall short. Data orchestration sees solutions ranging from relying on traditional SIMD processing [47, 42], architecting PEs to be small and easy to keep active [5] or complex software programmed networks at the core-level to deliver data to compute units [38]. Data movement is typically solved by the interconnection on-chip – some use a packet-switched NoC to make data movement entirely dynamic [47, 38], some introduce multicast primitives atop a traditional NoC [42] while others use an entirely statically configured NoC, moving the task of data movement entirely to software [5]. In some cases, relatively good balance of data orchestration and movement is achieved, for example, Simba [42] and Sigma [38]. However, Simba is designed as an inference-only accelerator, and Sigma only evaluates GEMM operations. Table 1 summarizes these works, as well as whether each of these four problems are solved by primarily software, hardware, or unaddressed.

Table 1: Summary of related work’s solutions to DL acclerator challenges.

Architecture	Work Place.	Data Mov.	Data Orch.	Cov.
NVIDIA GPU	HW	HW	HW	Yes
Simba (2019) [42]	SW	HW	HW	No
EyerissV2 (2019) [5]	SW	SW	HW	No
MAGNet (2019) [47]	SW	HW	HW	No
SIGMA (2020) [38]	SW	HW	SW	No
Violet	SW	HW	HW	Yes

In this work, we develop a novel accelerator architecture, Violet, with DL coverage as a first-order goal, achieving this through carefully balancing the responsibilities for work placement, data orchestration, data movement between the architecture, microarchitecture and compiler. Fine grained data orchestration is supported by extending traditional SIMD with an architecturally exposed transpose engine, enabling highly efficient execution of state-of-art DL workloads by reusing cache lines loaded from a core’s private data cache. Efficient data movement is tackled by extending a 2D mesh NoC to be a first-class programmable component in the architecture with the inclusion of a special data movement core. Flexible work placement is supported by the kernel-based execution model coupled with a dynamic, cache-based, memory system. Finally, coverage of DL applications is easily achieved as a result of our choice of balance lending to rapid software stack development – and this coverage is demonstrated by Violet’s ability to run all of the applications (inference and training) in the MLPerf benchmark suite.

Specifically, the contributions of this work are:

- A detailed qualitative and quantitative characterization of a broad set of DL applications and their imputed needs on the hardware/architecture. We evaluate 300+ different shapes of operators, across CNNs, Transformers, and LSTMs which as far as we know is the widest such study.
- A novel architecture, Violet, designed to balance the responsibilities of work placement, data orchestration, and data movement between the architecture and software-stack. We find that for data orchestration in particular, a narrow subset of AVX plus a small extension suffices.
- A detailed distillation of how Violet’s architectural features and balance of responsibilities enable Violet to be an easy compilation target across a broad set of DL workloads in addition to achieving competitive or superior performance compared to state-of-art industry solutions. We call out specifically what features of each operator can be leveraged by Violet’s exposed data orchestration and movement primitives.
- An analysis across DL applications, comparing Violet to the NVIDIA A100 GPU which shows Violet achieves 2.4X / 2.1X geo-mean speed-up at batch 16 size inference / training with 10.6X / 9.5X power efficiency.
- A deep dive into operator-shape level characteristics and

Table 2: Summary of key behaviors in DL operator shapes.

#	Behavior
1	Large-channel convs. that map well to GEMM units
2	Large-spatial convs. that give easy parallelism
3	Unit-filter convs. which are just matrix multiply
4	Conv. backpropagation which is hard to parallelize
5	Choice of tiling can impact comm. via placement
6	Large matmuls. that are easy to get high perf.
7	Odd-shaped Batch matmuls. hard data orch.
8	LSTM with low parallelism

behaviors across MLPerf. In particular, we distill out 8 key behaviors which have generalizeable implications beyond just our proposed design, and could even be used to help improve GPUs. Table 2 summarizes the key behaviors.

The rest of this paper is organized as follows. Section 2 explains further the related works to this paper and our differentiation from contemporary DL accelerator designs. Section 3 overviews and analyzes DL applications, providing a broad set of workload behaviors and how they frame the four key problems for bridging the gap. Section 4 presents Violet, a novel architecture for DL acceleration that achieves high performance and coverage of state-of-art DL apps in the MLPerf benchmark suite. Section 5 shows how Violet’s balance of responsibilities and solutions to the four key problems make it possible to rapidly produce performant mappings of dominant DL operators. Section 6 describes our methodology for evaluating Violet. Section 7 presents our evaluation, where we explore the design space of Violet, its performance and efficiency compared to the A100, the key application behaviors of MLPerf operators that afford this performance, as well as a limit study on the possible future improvements for Violet.

2. Related Work

Violet Positioning. Within the space of platforms for DL, general purpose processors (GPP) are one end, achieving low performance, high coverage and easy compilability; GPUs are in the middle achieving high performance, efficiency, coverage and good compilability by adding specialized units to an existing flexible architecture; DL accelerators use exotic architecture, aspiring for extreme performance efficiency, and have thus far sacrificed generality and make compilability hard [42, 5, 38, 47]. Table 3 summarizes these observations. As argued in [41, 15], compilability – the ease in which DL operations can be lowered to an architecture – is a fundamental requirement to usability. This work explores the GPP paradigm to answer whether we can get higher efficiency than a GPU while also providing compilability. REDUCT [34] is the closest *philisophically* related work to Violet.

DL Accelerators. There are many proposed designs for DL acceleration [5, 38, 42, 47]. These architectures are all based on an array of PEs which contain structures optimized for multiply-accumulate (MAC) or GEMM operations (or SpMM

Table 3: Qualitative comparison of General Purpose processor, GPU and AI Accelerators.

	GP Core	GPU	AI Acc.
Efficiency	Low	High	Higher
DL Generality	High	High	Low
HPC Generality	High	High	Very Low
Compilability	Easy	Autotuning	Hard

Table 4: Summary of Violet’s differences to related work.

Architecture	Comments or differences to our approach
Simba	Chiplets, Special bufs, Inf. for CNN only
EyerissV2	Special PE, bufs, HM-NoC, Inf. for CNN only
MAGNet	RTL Gen., Special bufs, Inf. for CNN only
SIGMA	Specialized PE, DNN only

to exploit structured sparsity). EyerissV2 [5] uses a circuit switched, statically configured NoC, meaning software must plan all data movement at compile time. Further, the way in which this NoC is exposed architecturally is not examined and only configurations for convolution and matrix multiply inference are evaluated. Sigma [38] and MAGNet [47] both have similar system level architecture. They use a traditional 2D mesh, relying on packet-switched routing for data movement and carefully crafted work placement to optimize communication pressure. Sigma uses a custom PE design with software configured data orchestration. MAGNet uses a conventional SIMD-style compute unit. Sigma only evaluates matrix multiply workloads, constraining it to DNNs such as GNMT and Transformers. MAGNet only considers convolution inference, and is intentionally specialized this way. Simba [42] is designed to be a small-batch inference accelerator based on chiplets, with a mesh NoC on each chiplet, and mesh NoC on the whole package. Simba also has a “Global PE” for near-data operations but only this one compute component is able to perform this kind of work. Table 4 summarizes the differences between these works and this paper.

SIMD Architectures. There have been recent works on SIMD and in particular, looking at AVX extensions. These include REDUCT [34], analysis of convolution performance [13], and analysis of inference on CPUs [31]. Mittal et al. [33] presents a survey of deep-learning on CPUs and focus on issues of memory hierarchy and datapath. Domke et al. [11] present a thoughtful case to understand and revisit the role of Matrix Engines for HPC. Reuther et al. present a survey on DL accelerators [40]. These works do not look at the details of program behavior, contribution of architecture, or DL coverage. Google has published an extensive set of papers on TPU including [23], which cover the software stack, systolic array architecture, and datatypes.

DL Application Analysis and Software Techniques. Verma et al. present a workload characterization of MLPerf Training [48]. Cross-layer approaches related to our work include

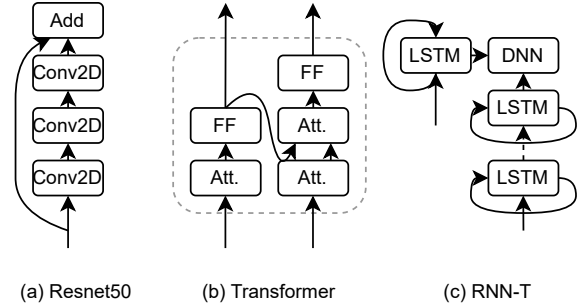


Figure 2: Overview of Common DL Applications

high- [43] and low- [27, 53] level code generation techniques, and also memory management [19] and memory partitioning techniques [30, 44, 21]. Operator mappers which design dataflows for operator shapes employ techniques such as loop ordering and search [37, 29, 20], intrinsic mapping [53], template-based [13, 25], and manual programming [6, 14].

3. Characterization of DL Applications

This section provides an overview of deep-learning applications focusing on distilling the program behaviors and the implications on the four DL accelerator challenge problems.

3.1. An Overview of a DL Application

Deep learning applications are computer programs which operate over *tensors* – multidimensional arrays. Tensors are either *fixed* or *learned*. Fixed tensors are given (unchangeable) inputs to a network, and learned tensors are called *parameters* or *weights*. During the execution, a directed acyclic graph (DAG) is constructed where nodes are operations, and edges are the tensors that are consumed or produced by that operation. This *compute graph* represents the dynamic instance of computation performed by the application, and serves as the input to the automatic differentiation (autograd) algorithm to compute compute gradients of every tensor with respect to a given output (the “loss” value). The initial execution of the program and construction of the compute graph is referred to as *inference* or the *forward pass*. Autograd, and gradient computation is often referred to as *backpropagation* or the *backward pass*. Both forward and backward passes together are referred to as *training*. DL applications produce the same compute graph for any input. These applications can be captured by its compute graph alone¹. Figure 2 shows the compute graph for several example DL applications. Most DL applications are implemented using frameworks such as Tensorflow, PyTorch and ONNX. These frameworks, in addition to providing implementations for operators, handle automatic differentiation. To support new architectures, the onus is on the accelerator designer to lower framework-level operators to their architecture,

¹In some well behaved, non-static cases, such as recurrent networks, we can still capture the compute graph by introducing cyclic edges. These are called “quasi-static”.

Table 5: Summary of different properties of workloads

Network	GOPs	Shapes	Primary Ops	%
RN50	8	23	Conv2D	99%
SSD	427	30	Conv2D	99%
UNET	938	18	Conv3D	99%
BERT	110	5	MatMul	98%
RNNT	14	6	LSTM, MM	94%
RN50	24	69	Conv2D	99%
SSD	83	90	Conv2D	99%
UNET	2816	54	Conv3D	99%
BERT	479	15	MatMul	98%
RNNT	42	14	LSTM, MM	94%

creating a substantial software lift necessitating compilability as a first order requirement

3.2. Characterization and Implications for Hardware

From a computer architecture perspective, the operations’ semantics, their execution order, as well as tensor **shape** (dimensions), **layout** (the order in which these dimensions are flattened in memory) and **datatype** play a role in data orchestration, data movement and work placement. Here we characterize the entire MLPerf suite and detail how these characteristics impact these problems. Table 5 summarizes the quantitative features of each of the applications. Based on qualitative understanding of the applications and detailed quantitative profiling (methodology explained in Section 6), our general findings are below.

Operators and Application Coverage. Across the MLPerf suite of applications, three operators dominate: matrix multiply, convolution, and LSTM, accounting for over 90% of all ops in each network. For these three, over 300 unique shapes exist with various amounts of arithmetic intensity, available reuse, layouts, intermingling with elementwise operations such as ReLU, batchnorm all with different variations for forward and backward pass. This means any solution for coverage directly depends on its solutions for work placement, data orchestration and data movement across the set shapes to be supported. In addition, while focus can be placed on these operations, an architecture needs to be balanced to support the range of DL operations needed (E.g. Batch Norm, Layer Norm, Softmax) otherwise it will be limited by Amdahl’s law at best, or be unable to achieve DL application coverage at worst. *A good solution to DL coverage is a composite of solutions to data orchestration, data movement and work placement, and how these solutions generalize.*

Layout and Datatype drives Data Orchestration. Tensor layout directly impacts which dimensions can be used for vectorization and what minimum tiling factors are needed. For some datatypes (Integer as well as Float16), multiply-accumulates use a wider datatype for accumulation. For example, Intel’s recent AVX extensions support an Int8 to Int32 multiply-accumulate [10]. On the hardware side Int8 to FP16 costs 3X in area, up to 5X in power, while Int8 to FP32 costs

10X to 20X in area and power [1, 22, 52, 12]. *A good solution to data orchestration must be aware of, and be performance-agnostic to layout or datatype, and in the process, avoid introducing needless software or hardware complexity. Care must also be taken to balance data orchestration tiling needs with work placement parallelization needs (explained below) to achieve maximum utilization.*

Reuse drives Data Movement. Arithmetically intense DL operations (all three of our dominant operators typically have high arithmetic intensity) afford a lot of data-reuse opportunities – and for most DL operations, data-dependencies are entirely statically defined. In addition, having a static (or quasi-static) compute graph allows operations to be executed in topological order. This means that often the output from one operation will be immediately used in the next operation leading to an obvious temporal locality of tensor operands. *A good solution to data movement must be able to recognize and exploit available information on data dependencies and reuse. While it may seem intuitive to solve entirely with software, this approach is typically involves leaking microarchitectural constraints to the software creating performance pitfalls when trying to generalize. Balance must be struck between data movement and application coverage.*

Parallelism drives Work Placement. The amount of and ease in exploiting available parallelism are the key factors which impact work placement. The three dominant operators we observe all have ample parallelism. In addition, for inference, batching of multiple inputs provides higher reuse and more embarrassing parallelism, with almost no additional pressure on the hardware. **Training with large batches, provides the same, but a linear increase in the amount of intermediates that need to be kept-around, before the backward pass can commence, meaning larger memory capacity is needed resulting in higher total dollar cost as well as higher memory power.** Work placement also directly impacts data movement – units of work which share input data are best placed physically proximate to each other to ease the burden on data movement and allow it to extract out broadcasting opportunities. *A good solution for work placement should support coverage by abstracting microarchitectural constraints, strategically exposing constraints when critical for data movement. It should also afford tuning placements for extracting additional performance with expert knowledge.*

4. Violet Architecture

In this section we detail the design of Violet, a novel architecture with roots in multi-core SIMD, for generalized deep learning acceleration. We first overview the organization of Violet, then explain in detail how Violet’s design solves the four problems of data orchestration, data movement, work placement and application coverage.

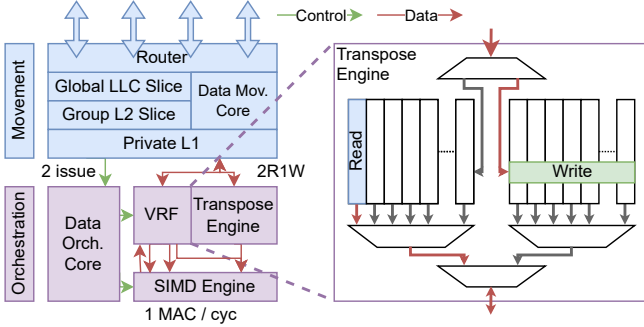


Figure 3: Organization of Violet Tile.

4.1. System Organization

Violet, shown in detail in Figure 1 and Figure 3, consists logically of three main components: 1) Parallel processing elements 2) An interconnection network and 3) A memory system. Physically, Violet is divided into identical tiles, each containing a data orchestration core coupled with a wide SIMD/short-vector datapath including register file and arithmetic units organized as lanes². The tile also contains a slice of a distributed memory hierarchy over a 2D mesh NoC combined with a data movement engine. We find the mechanics of the ISA are unimportant as suggested by Blem et al. [3].

The system includes a global thread scheduler that transmits work to cores based on software-defined work placement. It also includes a host interface controller (PCIe-like interface) to provide high bandwidth, low latency communication to a general purpose host computer that runs the system-level portions of the DL stack. Finally, one or more memory controllers and PHY on chip (HBM from a implementation standpoint is preferred) feed the LLC. The physical organization of the LLC is straight-forward: slices distributed across the chip with static address mapping³. A 2D-mesh interconnection network transmits cache lines between tiles and to and from memory.

4.2. Data Orchestration

Data orchestration concerns how the compute resources of an accelerator consume data and map it to execution resources. Quantitatively, data orchestration is solved *well* if compute resource utilization under *ideal memory* conditions is high. Violet’s SIMD datapath supports a small set of conventional SIMD instructions: add, multiply, multiply-accumulate, vector load/store (with broadcast & stride), wide-accumulate. In addition, we introduce a transpose engine, a novel microarchitecture component, which exposes custom vector instructions for loading transposed 2D blocks of vector elements while maintaining memory throughput. Section 5 further explains the use and benefit of the transpose engine. The transpose engine relies on minimum block size to amortize cache-line loads over the number of resulting SIMD vectors it produces. We synthesized the transpose engine in RTL to confirm the

²From here on, we use SIMD, SIMD Register-File and SIMD lane

³Tensor layout can be optimized to fine tune proximity of slices to cores

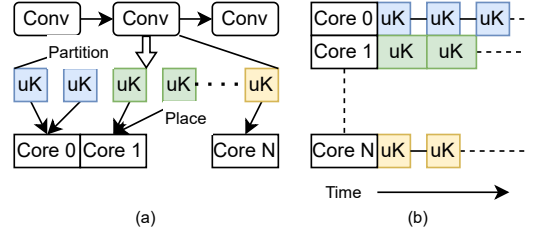


Figure 4: Execution model and lower of graph to hardware primitives. (a) Shows how DL operators are lowered down to low-level primitives. (b) The execution model of an operator.

designs feasibility. One SIMD lane supports two Int8 and one FP16 multiply-accumulate operation per cycle. It allows internal accumulation in 32-bits. The size of the architectural register file and SIMD lanes is a first-order determinant of performance, since it dictates how much parallel work can be done before hitting WAW hazards. We found that with 32 registers, MLPerf applications can be supported without the core becoming the bottleneck.

4.3. Data Movement

Data movement concerns how data needed for computation is moved from storage (typically, external DRAM) into the compute resources. Quantitatively, data movement is solved *well* if end-to-end compute resource utilization under *ideal compute* conditions is high. Violet addresses data movement by combining a traditional memory hierarchy with a special communication interconnect that includes a programmable data movement engine. This programmable network allows software to facilitate a “push”-style of prefetch operation, where the LLC essentially can “push” data to destinations over the network automatically (and without software planned routes), eliminating request traffic. The rich information in DL stacks allow such static analysis to be effective and straightforward (unlike codebases like SpecINT, SpecFP etc.). The three-level hierarchy of our memory system and L2 group sizes are chosen to enable the data movement engine to specify all destinations in the packet header, allowing the NoC and routing algorithm to intelligently multicast cachelines at any router, reducing network traffic to transmit a cacheline. In addition to this, Violet is able to support work that operates directly on the local LLC slice in a tile, meaning element-wise operations do not require data movement at all. The tile’s private cache is sized to be 32 KB as a staging area for data.

4.4. Work Placement

Work placement describes how an operation’s work is allocated to available resources on the architecture. A placement solution must often be spatially aware to understand what placement options are best for spatial data locality (and thereby improve data movement efficiency). It must also be aware of the details of the memory system (coherence, consistency, etc) as well as the execution model, to understand what work is

allowed to be placed on what resources. For the purposes of work placement, Violet can be viewed as a parallel thread array with one thread per core, with incoherent memory between physical cores. To lower an operator to Violet, a programmer or software *partitions* work for a given operator into individual tasks, each of which run on one logical thread. They then *place* this work onto the available cores with goal to map tasks with overlapping sets of data onto the same core (to ease data movement) while also balancing parallelism. Figure 4 provides a pictorial representation of this process.

5. Demonstrating Coverage

For Violet to achieve coverage of DL applications and demonstrate the compilability of Violet, we developed techniques for mapping and lowering the primary operators from MLPerf, paying close attention to the role of Violet’s novel transpose engine and programmable interconnect in achieving high performance and developer user experience.

We adopt output-stationary dataflow as a baseline strategy. This lends to an easy to understand parallel algorithm in that it eliminates inter-thread communication, leaning on “push” prefetch and dynamic multicast to exploit load-reuse opportunities, and the transpose engine to deliver performant data orchestration. Work items are sized to optimize for arithmetic intensity, respecting minimum tiling parameters to fill the SIMD+Transpose unit, as well as L1 data cache size. For each operator, we develop a micro-kernel which handles a single output chunk. Figure 5 shows an overview of operator mapping for two representative operators: convolution and matrix multiply. It shows the highest level operations in terms of the two tensors, the chunking to achieve parallelism, reuse available, and the lowest-level code snippet. We now explain each operator’s mapping in more detail, calling out the key details which Violet leverages to achieve high performance and efficiency without a complex software lift.

Matrix Multiply. Linear layers in DL applications are implemented as a matrix multiply of two input matrices A and B which have shapes $A[M, K]$ and $B[K, N]$ (B is typically the “weight” tensor). We base our strategy on NGemm [2], taking into account the effects of wide-accumulation for integer datatypes. Each output chunk can itself be computed as a matrix multiply of slices of the original A and B , and the minimum size of these chunks is dictated by which dimensions are vectorized over and by how much. Violet’s Transpose Engine allows for a special type of “transposed-load” which allows a number of cache lines to be loaded with their data then striped across many transposed vector-registers. The number of cache lines loaded is equal to the vector width (in bytes) divided by the ratio between the input and accumulation datatypes (4 in the case of Int8->Int32 matrix multiply). **This special transposed-load is employed to reduce the number of cache line loads needed to fill vector registers with relevant data by exploiting spatial locality in the algorithm. The exact layout combination**

– that is, whether A, B, both, or neither are transposed themselves – impacts how transposed-loads are employed and ultimately, the minimum tiling factors needed for sustained throughput. Figure 6 depicts the use of a transposed load (VLD4T) and a broadcast load (VLB4X4, similar to vbroadcastss in AVX-2) to fill vector registers to be used in a multiply-accumulate operation.

From another perspective, using the transpose engine changes the semantics of the SIMD MAC from VL-dot products of size 1 to (VL/R)-dot products of size R ($R=4$ for Int8, $R=2$ for Float16). This allows a tradeoff between the minimum K needed and minimum N needed in order to hide memory loads behind vector MAC operations. In the case of MKKN layout in Figure 6, if we have $T_M = 16$, $T_N = 4$, $T_K = 16$, we are loading 16 cache lines from A, 4 cache lines from B, and performing 16 vector MACs. With Violet’s dual read-port cache, we can cover the 10 cycles needed to load cachelines behind the 16 vector MAC operations. The work placement algorithm we employ for Violet understands this tradeoff and is able to select which minimum tile is better for a given shape.

Data movement of input slices to a core is part of the microkernel specification. A mechanical process is employed to enumerate the slices needed by each core across the timesteps of execution and generate a data movement program which pushes relevant data in the local LLC and L2 slice to each of the consumers that need it.

Back-propagation is also a matrix multiply operation, multiplying the output gradient by the original two inputs in two separate operations – and in each case, the layout of one of the tensors is transposed. So for a forward pass that is MKKN, the backward pass will observe layouts of KMKN and MKNK. We similarly can choose min. tiling factors based on what is needed to cover cache line loads with vector MAC operations. **Convolution.** We implement convolution based on Intel’s approach [13]. We similarly adopt an output-stationary dataflow. Each output block is computed by invoking a small GEMM kernel over the input and filter, with the reduction dimension being the input channels of the convolution. **Because the microkernels for convolution are small matrix multiplies, we can reuse the same analysis for matmul to define minimum tile sizes for maximum compute throughput.**

For computing convolution input back-propagation (dI) and weight back-propagation (dW) we follow a similar approach to designing an algorithm – employing our small matrix multiply algorithm to compute output chunks for these two operations. Weight gradient computation has to reduce over spatial dimensions, so there is little available parallelism. We adopt a similar strategy to [13] in this case, applying some tiling factor to the batch dimension and computing partial gradients over this tiling factor. We then apply a reduction kernel to sum the partial gradients. Using Violet’s ability for core to operate directly out of the LLC, we are able to perform this reduction without incurring any additional communication cost.

LSTM. The LSTM blocks in RNN-T decompose into two

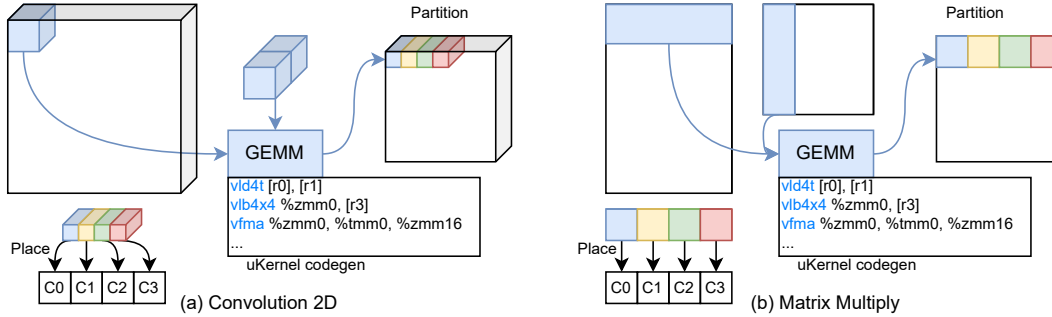


Figure 5: Mapping of Common Operators to the Violet architecture

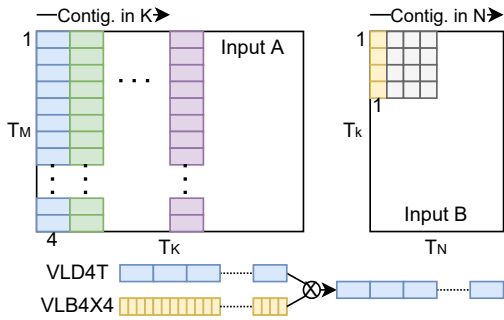


Figure 6: Use of transposed-loads in a small matrix-multiply.

very nice operations: a matrix multiply, and an element-wise operation. The matrix multiply is for the linear layer that transforms the input and hidden state for the current time step of the LSTM. The LSTM operation, past this linear layer, is elementwise over the vector elements of the input and hidden state. **We employ our high performance matrix multiply algorithm to handle the linear layers, then use the same in-LLC compute to handle the LSTM Cell’s element-wise computation.** Backpropagation is quite simple in that it just requires an element-wise gradient operation for the LSTM computation, and then a matrix-multiply backpropagation which we can reuse the algorithm from before.

5.1. Compiler and Software Stack

Violet’s software stack is positioned to support a DL-framework level abstraction. At the top level is TensorFlow and PyTorch which issue calls to allocate and transfer memory, and execute operators. Our software stack is made up of a runtime component which handles memory management and device excution, and a library component which contains operator code templates that are specialized just-in-time based on operator shapes. These templates are stored in a domain specific language that separates out the mapping task into low-level code-generation and work placement. Code-generation is handled by a conventional compiler, while work placement is handled by the above strategies. The architecturally exposed mechanics for data orchestration and movement can be lowered to easily by this template-based approach. Thus, we address the compilability challenge that plagues other designs.

6. Methodology

We now detail our evaluation methodology of end-to-end DL applications implemented in TensorFlow/PyTorch.

Performance Modeling. We insert region markers into TensorFlow and PyTorch at the operator boundary to generate an operator trace. For performance evaluation, we build a Zsim-like performance simulator/model that uses the DL operator trace, and a memory system model, accounting for the effects of the vector instructions, access rates to private memory, as well as NoC contention.

Power and Area Estimation. We used the methodology in Accelergy [50] and Timeloop for our area and power modeling. We use the LX3 processor core mentioned in [35, 17] as a reference for the power and area of a lightweight, in-order core. Ara [4] provides an estimate of SIMD area and power. We use the arithmetic units from [22] as a reference for the SIMD MAC unit. Finally, Cacti is used for power and area estimates of the last level cache. All of these components are normalized to 7nm power and area using the methods from [45]. The power consumption of the memory controllers, PHY and HBM stacks is 6 Watts per stack (24W for entire chip) based on data sheets for HBM2. For frequency scaling, we make use of work presented by ARM on their Neoverse N1 CPU, which presents power scaling for 3 GHz to 1.2 GHz [7].

Baseline and Comparing Performance. To report our results, we obtained published performance results of the NVIDIA A100 system. We paid close attention to ensure that we were using the exact same DL-model as the NVIDIA system. For some applications, we used NVIDIA’s code published through MLPerf to replicate performance results and obtain results for different batch sizes. For Bert Large pretraining, we were unable to run NVIDIA’s official code on a single GPU so we used the ratio of large batch inference to small batch inference to estimate small batch pretraining. To obtain layer-level performance and efficiency, we ran individual operators with PyTorch on an A100 and collected runtime using NVIDIA NSYS, computing utilization with FLOP counts for each layer.

Limitations. We focus on an execution model of one operator active at a time – leaving inter-operator parallelism for future work. As described in the results, this simpler approach

provides substantial performance and efficiency already. Also, we focus on single-node training, with the observation that techniques for high-performance distributed training are orthogonal to single-node performance. Klenk et al. show that perfect all-reduce improves performance by 10% to 40% [28]. Finally, we present qualitative comparison to existing academic designs since they don’t support many of the operators in MLPerf for full application execution and comparison, precluding a “fair” quantitative comparison against them.

7. Results

We evaluate Violet across the MLPerf benchmark suite, gathering detailed performance and power data at an operator level granularity. The results of our study are organized as follows. Sec 7.1 introduces Violet’s design space, examining what design parameters have the biggest impact on overall performance. Sec 7.2 presents a comparison of our chosen configuration, Vi2048, to an NVIDIA A100 GPU – a state-of-art DL accelerator – showing how Vi2048 can achieve superior performance and power efficiency. Sec 7.3 dives deeper into the operator shapes which have the highest impact on run time for each workload, distilling how the balance of responsibilities for data orchestration, data movement and work placement help enable high performance on each shape. Sec 7.5 presents a scalability study, examining the effects of optimizing different components of Violet, for the purpose of elucidating where the bottlenecks are, and what components should be focused on for further improvement. **We evaluate the entire 300+ unique operator shapes in the MLPerf application suite, extracting out performance and efficiency characteristics.**

7.1. Design Space Exploration

We first conducted an in-depth analysis of the design space that is created over the parameters of SIMD-width, number of processing cores, and frequency. We used our model to plot all of the design points in our space in terms of their area efficiency (TOPS / mm^2) and power efficiency (pJ / OP). Figure 7 shows the results of this survey. We can see that there is quite a diverse spread of design points that vary by up to a factor of 3X in terms of area efficiency, and 4X in terms of power efficiency. Further, we observe that not all applications agree on which design point is the most efficient overall.

To elucidate efficiency, we search design space and consider only points that match peak performance of A100. This allows us to look at utilization, speedup and perf/watt as metrics to evaluate underlying the efficiency of the architecture. For each application, we then identified the best configuration in terms of power efficiency, and then in terms of area efficiency to break ties. The result was Vi2048 – 2048 cores, 512-bit SIMD, at 2.4GHz operating frequency. We also observe that Vi2048 comes within 20% of the optimal TOPS/ mm^2 and within 25% of the optimal pJ/OP for each applications, with the exceptions of 50% for BERT and RNN-T large batch training.

Table 6: Comparison of Specs.

Spec	Vi2048	A100
Die Area	215 mm^2	840 mm^2
Peak TOPs (Int8/FP16)	524/262	624/312
Power (TDP)	100 W	300 W
Frequency	2.4 GHz	1.4 GHz
Total L1/L2/LLC Size	64/32/128 MB	20.25/-/40 MB
HBM2 Memory	16 GB	40 GB
# HBM2 Stacks	2	5
Est. \$-cost	\$263	\$866

Note: We rename NVIDIA’s L2 to LLC to compare with Violet.

7.2. Comparison to A100

We now compare the Vi2048 implementation, against an NVIDIA A100 GPU. We choose a relatively small batch size of 16 to contain the need for the high memory bandwidth and dollar cost of large batch training and also to stress Violet capability of extracting out parallelism when batch-level parallelism is low⁴. Table 6 shows a spec comparison of Vi2048 to the A100. We build a simple cost model based on wafer/die costs published here (\$238 for 600 mm^2 die) [26] and publicly available information on GDDR6 chip cost (roughly \$90 for 8GB) [9], and assume optimistically for A100 (that HBM costs the same). This indeed ignores cost of interposer, packaging etc. Figures 8 shows the comparison of performance. **Overall, Vi2048 achieves 2.4X / 2.1X geo-mean speed-up at batch 16 size inference / training with 10.6X / 9.5X power efficiency.** We intentionally picked a design point that was iso-performance to the A100. **This makes clear the speedup we see with Vi2048 comes from improving the utilization of compute resources by the same factor, with almost an order of magnitude lower energy. Energy efficiency of U2048 is much higher, because we rely on power-efficient microarchitecture targeted to DL exploiting reuse, data movement and orchestration, vs. a GPU that must adhere to a throughput-optimized execution model that constantly moves values in and out of main memory.**

To highlight the scope of Violet’s design space and flexibility, a chip optimized for transformer training would result in having 4096 cores, 512-bit SIMD, operating at 2.4GHz. This ViTr configuration is able to improve the energy efficiency gain over A100 from 6.3X to 8X for BERT training.

7.3. Operator Analysis of MLPerf App Performance

We now dive deeper into each application by conducting a layer-wise analysis of MLPerf and extract out and analyze important, architecture-agnostic behaviors. We also discuss how Violet is able to achieve high performance given these behaviors. Table 7 summarizes our findings for the top 3-5

⁴At batch size 16, A100 utilization is less than 1% for RNN-T, skewing our results, so we choose batch size 512 for RNN-T. Also, RNN-T’s recurrent architecture lends to a small model size which afford very large batch execution without exorbitant memory and bandwidth needs.

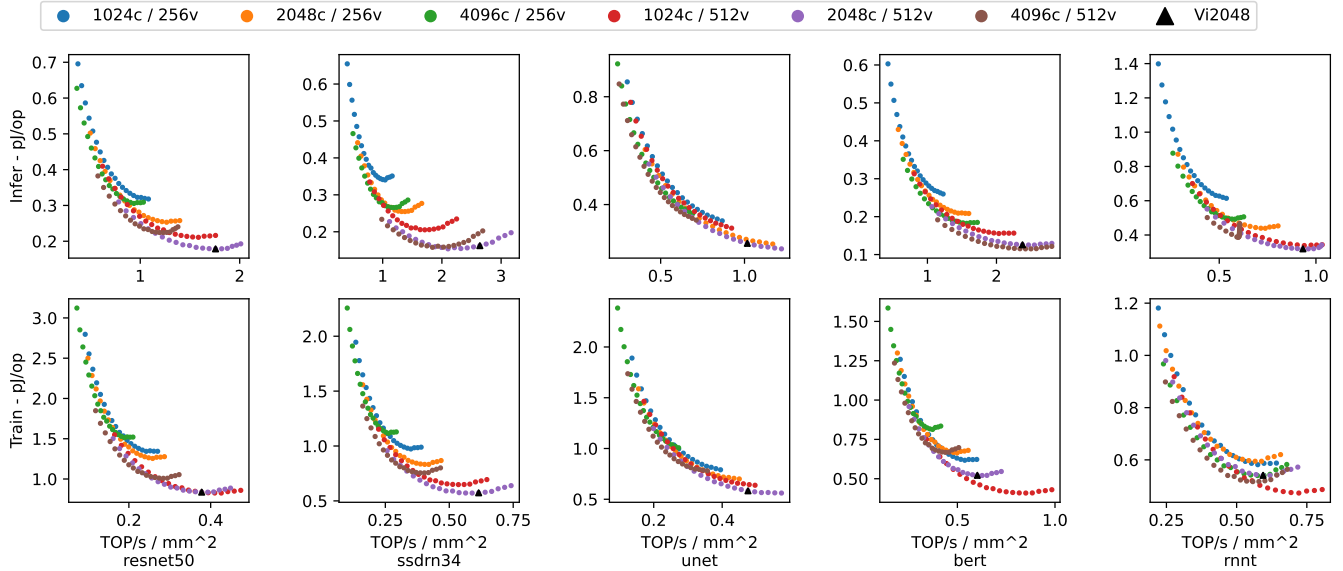


Figure 7: Design Space Exploration of Violet. Points of same color sweep from 1GHz-3GHz clock frequency with steps of 100MHz.

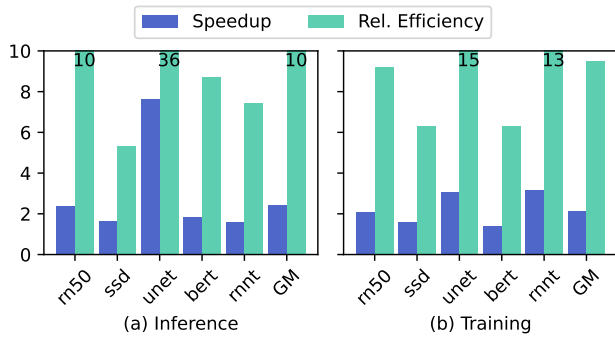


Figure 8: Violet vs A100 across MLPerf at batch size = 16. Throughput in samp/sec, and Rel. Eff. is ratio of avg. pJ/op.

operator shapes in each network by percentage of total op count. Each row is one (I) inference or (T) training layer of the network with utilization as a percentage of peak compute throughput for Vi2048 with the Transpose Engine enabled (+TP), with the Transpose Engine disabled (-TP) and for the A100. The symbols we use have the following meaning. $\underline{LC/SC}$, $\underline{LS/SS}$: Large/Small Channel, Spatial Conv. $\underline{F1}$: Filter size = 1 Conv. \underline{DW} : Conv. backprop for weights. \underline{BP} : Bad placement caused by tiling. $\underline{LM/SM}$, $\underline{LN/SN}$, $\underline{LK/SK}$: Large/Small M, N, K matmul. \underline{TP} : Transposed matmuls for backprop. \underline{EW} : Elementwise operations. **We identify the fundamental application behaviors that are key to achieving high performance and efficiency. The identification and explanation of these behaviors are a contribution that is architecture agnostic and to our knowledge, the most comprehensive such analysis.**

1. Large Channel Convolution. convolutions have a large channel \underline{LC} dimensions, making inner matrix multiplies amenable to both Violet’s SIMD unit and A100’s TensorCore.

Often channel dimensions are large enough that Violet’s transpose engine becomes unnecessary for performance. When spatial dimensions are small \underline{SS} , additional parallelism is extracted from output channels, putting more pressure on the transpose engine. In this case, we also observe that the A100 suffers in utilization; likely due to the fact the inner tile dimensions end up not filling the relatively large TensorCore.

2. Large Spatial Convolution. convolutions have high parallelism from splitting work on spatial dimensions \underline{LS} , as exemplified by UNET’s large spatial convolutions. We can also see the A100 appears to require both large spatial and channel dimensions to extract high utilization – both L11 and L21 have a large amount of spatial parallelism available, but L21 has much smaller channel count, which is likely why A100’s performance suffers.

3. Unit-Filter Convolution. convolutions with one filter pixel $\underline{F1}$ degenerate into a large matrix multiply (M = spatial dimension, N = output channel, K = input channel). In this case, Violet is able to perform quite well even without the transpose engine since typically channel dimensions are large. When $M \gg N$, we find that communication becomes the bottleneck since arithmetic intensity drops.

4. Convolution Backpropagation. Backpropagation for convolution is difficult for two reasons: 1) matrix multiply layouts are transposed, altering minimum tiling requirements, and 2) backpropagation for weights \underline{DW} cannot parallelize on spatial dimensions. With this parallelism gone, Violet relies on the channel dimensions, and when this is insufficient, partial gradients are computed over the batch dimension and summed together with in-LLC reduction as discussed in Section 5. It is likely that A100 suffers from a similar problem.

5. Tiling Effects on Placement. In some cases \underline{BP} , we observe a decrease in efficiency when using the transpose engine

Table 7: Analysis of Top 3-5 layers for each app. by op count

Op	+TP	-TP	A100	Comments
Resnet50 (All 2D Conv.)				
I 14 ² 256->256 f=3 s1	82	68	14	<u>SS LC</u>
I 56 ² 64->64 f=3 s1	90	78	12	<u>LS SC</u>
I 28 ² 128->128 f=3 s1	80	82	16	<u>SS</u>
I 14 ² 256->1024 f=1 s1	69	93	8	<u>F1 LC A-</u>
I 14 ² 1024->256 f=1 s1	66	72	9	<u>SS BP</u>
T 14 ² 256->256 f=3 s1	25	5	15	<u>DW SS</u>
T 56 ² 64->64 f=3 s1	61	6	11	<u>DW LS SC</u>
T 28 ² 128->128 f=3 s1	65	6	14	<u>DW LS SC</u>
T 14 ² 256->1024 f=1 s1	34	15	8	<u>DW F1 LC</u>
T 14 ² 1024->256 f=1 s1	67	16	9	<u>DW F1 LC</u>
SSD-Resnet34 (All 2D Conv.)				
I 150 ² 256->256 f=3 s1	94	46	53	<u>LS LC GP</u>
I 150 ² 128->128 f=3 s1	97	82	37	<u>LS LC</u>
I 300 ² 64->64 f=3 s1	99	74	26	<u>LS</u>
I 150 ² 128->256 f=3 s1	98	67	43	<u>LS LC</u>
I 150 ² 256->512 f=3 s2	77	17	45	<u>S2</u>
T 38 ² 256->256 f=3 s1	53	5	37	<u>DW SS LC</u>
T 38 ² 128->128 f=3 s1	62	6	20	<u>DW SS LC</u>
T 75 ² 64->64 f=3 s1	69	6	14	<u>DW SS LC</u>
T 38 ² 128->256 f=3 s1	45	6	27	<u>DW SS LC</u>
T 38 ² 256->512 f=3 s2	25	3	27	<u>DW SS LC</u>
UNet (All 3D Conv.)				
I 32 ³ 32->32 f=3 s1	24	49	22	<u>BP LS SC</u>
I 32 ³ 64->32 f=3 s1	24	99	15	<u>BP LS SC</u>
I 32 ³ 64->64 f=3 s1	49	99	28	<u>BP LS SC</u>
I 32 ³ 128->64 f=3 s1	49	99	35	<u>BP LS LC</u>
I 32 ³ 128->128 f=3 s1	99	99	53	<u>BP LS LC</u>
T 32 ³ 32->32 f=3 s1	27	8	16	<u>DW LS SC</u>
T 32 ³ 64->32 f=3 s1	39	8	19	<u>DW LS SC</u>
T 32 ³ 64->64 f=3 s1	57	8	35	<u>DW LS SC</u>
T 32 ³ 128->64 f=3 s1	71	8	43	<u>DW LS LC</u>
T 32 ³ 128->128 f=3 s1	94	8	57	<u>DW LS LC</u>
BERT-Large				
I Fc(2848x1024x1024)	87	76	32	<u>LM LN LK</u>
I Fc(2848x4096x1024)	91	31	93	<u>LM LN LK</u>
I Fc(2848x1024x4096)	90	52	31	<u>LM LN LK</u>
I Mm(178x178x64)	27	27	8	<u>LL SM SN</u>
I Mm(178x64x178)	14	14	6	<u>LL SM SN</u>
T Fc(4064x1024x1024)	83	14	95	<u>TP LM LN LK</u>
T Fc(4064x4096x1024)	83	14	47	<u>TP LM LN LK</u>
T Fc(4064x1024x4096)	83	14	93	<u>TP LM LN LK</u>
T Mm(254x254x64)	2	2	9	<u>TP LL SM SN</u>
T Mm(254x64x254)	5	5	17	<u>TP LL SM SN</u>
RNN-T				
I Lstm(512x4096x2048)	65	18	22	<u>EW LN LK</u>
I Lstm(512x4096x3072)	50	36	24	<u>EW LN LK</u>
I Lstm(512x4096x1264)	91	56	16	<u>EW LN LK</u>
I Lstm(512x1280x640)	48	65	6	<u>EW SK</u>
I Fc(512x1344x512)	46	71	11	<u>EW BP</u>
T Lstm(512x4096x2048)	41	11	19	<u>TP EW LN LK</u>
T Lstm(512x4096x3072)	41	11	23	<u>TP EW LN LK</u>
T Lstm(512x4096x1264)	36	11	16	<u>TP EW LN LK</u>
T Lstm(512x1280x640)	47	14	5	<u>TP EW SK</u>
T Fc(512x1344x512)	42	14	7	<u>TP EW</u>

Table 8: Analysis of related academic DL accelerators on basis of their efficiency when observed behaviors are present.

Behav.	Simba	EyerissV2	MAGNet	SIGMA
1,2,3	Med-Hi	Med-Hi	Hi	Hi
4	Unsup.	Unsup.	Unsup.	Lo
5	Var.	Var.	Var.	Var.
6	Hi	Hi	Hi	Hi
7	Lo	Hi	Lo	Med-Hi
8	Med	Unsup.	Unsup.	Med

Behavior #5 depends on shape, the architecture, and mapping strategy and so is difficult to say how tiling factors impact each design.

in Violet. In all cases we analyzed, this was not due to under-utilization of the SIMD engine, but instead the change in tiling factors as a result of using the transpose engine caused work placement to produce worse communication patterns. This is not a problem for Violet since we can either naively just switch off the transpose engine, or fine-tune the placement by adjusting tiling factors.

6. Large Matrix Multiplies. The top 3 layers for BERT are matrix multiplies with large M LM, large N LN, large K LK. These kinds of shapes are easy for both SIMD and TensorCore, so it’s not surprising that both A100 and Violet perform well. It does appear the A100 requires even larger dimensions than L31 (for example) to achieve peak throughput (L32, L33). Additionally, similar to convolution, backward passes for matrix multiply are also matmuls but with transposed inputs TP.

7. Odd-shaped Batch Matrix Multiplies. BERT’s self attention layers employ batch matrix multiplies with large outer L dimension LL and relatively small M SM and small N SN dimensions. For these matrix multiplications, 1) the outer batch dimension afford embarrassing parallelism at the expense of interconnect pressure due to drop in arithmetic intensity 2) small and irregular M and N dimensions make it difficult to extract further parallelism meaning Violet’s transpose engine has little effect and 3) layout for this matrix multiply cannot be tuned for inference since neither input is a stored weight.

8. LSTM with low parallelism. The LSTM layer can be thought of as a linear layer over both the input and recurrent state, followed by a relatively complex element-wise operation. Violet leverages previously discussed techniques for computing the matrix multiples in the linear layers efficiently. Violet additionally employs careful in-memory layout of tensors to allow for in-LLC elementwise EW operation – meaning the LSTM gates are all computed over local data in a tile’s LLC slice, requiring no data movement after the linear layers.

7.4. Qualitative Analysis of Academic Architectures

To conclude this study, we present a qualitative analysis of academic DL accelerator designs on whether they would perform well for each of these behaviors. Table 8 summarizes our findings, which we now break down for each of the four architectures we study. Note that these still suffer from the unaddressed compilability challenge.

Simba only evaluates linear layers but should be able to perform convolutions. Given a vector width of 8, it should perform most convs. in MLPerf well but without additional data orchestration features, will suffer for some shapes. Being inference-only, training convolution is unsupported. For similar reasons, Simba is likely to perform well for large matmuls, but suffer for the irregular batch matmuls seen in transformers. Simba is likely to perform just okay for LSTMs since it will rely exclusively on batch parallelism, and only its Global PE is able to do near-memory reduction operations. Overall, Simba’s dynamic NoC and multicast capability from some units make it amenable to easy data movement, in addition, work placement, but its fixed width SIMD units and lack of support for training cause it to fall short on coverage and performance of MLPerf.

EyerissV2 is also an inference engine focusing on convolution. It is likely to support convolutions in MLPerf quite well with its row-stationary dataflow, but does not support training. Since matmuls are a degenerate case of convolution, EyerissV2 should also support matmul layers, likely working well for large matmuls. EyerissV2 would also likely work well for the irregular matmuls in transformers since its PEs are very fine-grained, making data-orchestration much easier at the PE level. EyerissV2 does not support activation functions, though so would not be able to run LSTM ops. EyerissV2’s interconnect is statically programmed by software, and if the routing needs of an application exceed hardware resources, software will be unable to route data. Overall, EyerissV2 has good data orchestration at the expense of complex, software controlled data movement. It has no support beyond DNN and CNN inference, so falls short on DL coverage.

MAGNet is an RTL generator which intentionally echews coverage in order to attain the highest possible performance and efficiency for a single application. It employs conventional SIMD execution, meaning it suffers from the data orchestration problems as Simba, but should support nice convolutions and matmuls well, but will likely suffer for irregular batch matmul shapes. It employs a dynamic interconnect so data movement and work placement is a relatively easy lift for software, but without multicast or the ability to “push” data, though, it has to route requests as well as data. Overall, MAGNet was not designed for coverage, and lacks data orchestration and movement techniques to achieve high performance for irregular shapes, as well as the ability to perform training.

SIGMA’s FlexDPE is capable of very flexible data orchestration at the core level. The tradeoff is a relatively complex fan-out/in network to deliver elements to hardware execution units, which we find to be over-engineered for DL applications (as exemplified by MLPerf). It has a NoC similar to MAGNet. It will likely perform well for nice matrix multiplies and convolutions as a result. For conv. backprop., it will likely suffer since it cannot perform near-data reductions to reduce communication pressure. It’s performance for irregular matmuls will depend on whether the dimensions can fill the

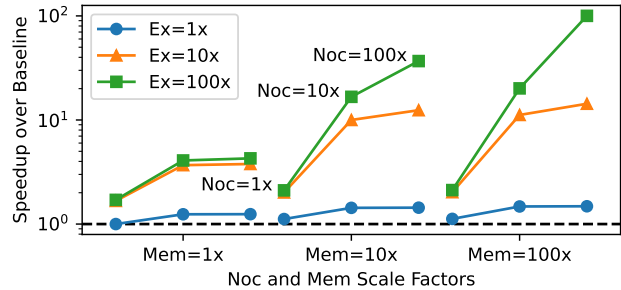


Figure 9: Overall performance sensitivity to Memory, Communication network, and Compute engine.

relatively large FlexDPE size. SIGMA will likely support LSTM operations about as well as Simba or A100. Overall, SIGMA has the highest coverage of the accelerators we study, but lacks architectural features for optimizing data movement, exacerbating its compilability limitation.

7.5. Violet’s Roadmap to the next 100X

To examine the scalability of Violet, we simulate the performance improvement from scaling each of compute, communication, and memory bandwidth by a factor of 1X, 10X, and 100X, separately and together (a total of 27 design points). Figure 9 shows these speedups normalized to Vi2048. The following insights emerge. **i) With additional memory bandwidth alone, at best 25% speedup is possible.** **ii) Conversely, since utilization is already high, improving memory bandwidth and NoC alone or together provides limited speedups.** **iii) Surprisingly, 10X in bandwidth and compute, with no change to the NoC, provides about 9X speedups, meaning the push-based NoC architecture scales.** Emerging packaging solutions could make this direction realistic to achieve. **iv) Getting speedups beyond 10X also seems surprisingly possible and not limited by application inherent characteristics.** Microarchitecture/architecture techniques that create an effective increase of 100X in memory bandwidth (main memory caches), fast NoCs (photonic like Corona [46]) could help realize these design points in a practical way.

8. Conclusion

This paper identifies the four key problems which must be solved for a new DL accelerator to be successful. Through a fresh perspective of extending established multicore SIMD architecture, we develop Violet, which solves these four problems in a balanced way, leading to high performance and coverage of modern DL applications. We provide a surprisingly effective approach that outperforms GPUs by large integer factors, with a substantially lower silicon footprint design. The analysis and key behaviors we identified are leveraged by Violet to achieve this, and have implications for future architectures as well.

References

- [1] Hamzah Abdel-Aziz, Ali Shafiee, Jong Hoon Shin, Ardavan Pedram, and Joseph H. Hassoun. Rethinking Floating Point Overheads for Mixed Precision DNN Accelerators. *arXiv:2101.11748 [cs]*, January 2021. arXiv: 2101.11748.
- [2] Wenlei Bao, Li-Wen Chang, Yang Chen, Ke Deng, Amit Agarwal, Emad Barsoum, and Abe Taha. Ngemm: Optimizing gemm for deep learning via compiler-based techniques. *arXiv preprint arXiv:1910.00178*, 2019.
- [3] Emily Blem, Jaikrishnan Menon, Thiruvengadam Vijayaraghavan, and Karthikeyan Sankaralingam. Isa wars: Understanding the relevance of isa being risc or cisc to performance, power, and energy on modern architectures. *ACM Trans. Comput. Syst.*, 33(1), March 2015.
- [4] Matheus Cavalcante, Fabian Schuiki, Florian Zaruba, Michael Schaffner, and Luca Benini. Ara: A 1-ghz+ scalable and energy-efficient risc-v vector processor with multiprecision floating-point support in 22-nm fd-soi. *IEEE Transactions on Very Large Scale Integration (VLSI) Systems*, 28(2):530–543, 2020.
- [5] Yu-Hsin Chen, Tien-Ju Yang, Joel Emer, and Vivienne Sze. Eyeriss v2: A flexible accelerator for emerging deep neural networks on mobile devices. *IEEE Journal on Emerging and Selected Topics in Circuits and Systems*, 9(2):292–308, 2019.
- [6] Sharan Chetlur, Cliff Woolley, Philippe Vandermersch, Jonathan Cohen, John Tran, Bryan Catanzaro, and Evan Shelhamer. cuDNN: Efficient Primitives for Deep Learning, December 2014. arXiv:1410.0759 [cs].
- [7] Robert Christy, Stuart Riches, Sujil Kottekkat, Prasanth Gopinath, Ketan Sawant, Anitha Kona, and Rob Harrison. 8.3 a 3ghz arm neoverse n1 cpu in 7nm finfet for infrastructure applications. In *2020 IEEE International Solid-State Circuits Conference - (ISSCC)*, pages 148–150, 2020.
- [8] Advanced Micro Devices Corporation. "amd instinct mi100" instruction set architecture. December 2020.
- [9] Aleksandar Cosic. Gddr5 vs gddr5x vs hbm vs hbm2 vs gddr6 vs gddr6x.
- [10] Alberto Cueva. Code Sample: Intel® AVX512-Deep Learning Boost: Intrinsic Functions, April 2019.
- [11] Jens Domke, Emil Vatai, Aleksandr Drozd, Peng ChenT, Yosuke Oyama, Lingqi Zhang, Shweta Salaria, Daichi Mukunoki, Artur Podobas, Mohamed WahibT, and Satoshi Matsuoka. Matrix engines for high performance computing: A paragon of performance or grasping at straws? In *2021 IEEE International Parallel and Distributed Processing Symposium (IPDPS)*, pages 1056–1065, 2021.
- [12] Bruce Fleischer, Sunil Shukla, Matthew Ziegler, Joel Silberman, Jinwook Oh, Vijavalakshmi Srinivasan, Jungwook Choi, Silvia Mueller, Ankur Agrawal, Tina Babinsky, Nianzheng Cao, Chia-Yu Chen, Pierce Chuang, Thomas Fox, George Gristede, Michael Guillorn, Howard Haynie, Michael Klaiber, Dongsoo Lee, Shih-Hsien Lo, Gary Maier, Michael Scheuermann, Swagath Venkataramani, Christos Vezytzis, Naigang Wang, Fanchieh Yee, Ching Zhou, Pong-Fei Lu, Brian Curran, Lei Chang, and Kailash Gopalakrishnan. A Scalable Multi-TeraOPS Deep Learning Processor Core for AI Trainina and Inference. In *2018 IEEE Symposium on VLSI Circuits*, pages 35–36, Honolulu, HI, June 2018. IEEE.
- [13] Evangelos Georganas, Sasikanth Avancha, Kunal Banerjee, Dhiraj Kalamkar, Greg Henry, Hans Pabst, and Alexander Heinecke. Anatomy of High-Performance Deep Learning Convolutions on SIMD Architectures. In *SC18: International Conference for High Performance Computing, Networking, Storage and Analysis*, pages 830–841, November 2018.
- [14] Gaël Guennebaud, Benoît Jacob, et al. Eigen v3. <http://eigen.tuxfamily.org>, 2010.
- [15] Linley Gwennap. GROQ ROCKS NEURAL NETWORKS. page 5, January 2020.
- [16] Linley Gwennap. QUALCOMM SAMPLES FIRST AI CHIP. page 3, 2020.
- [17] Tom R Halfhill. Xtensa LX3 and Xtensa 8 Cores Boost Performance, Cut Power. page 9, 2009.
- [18] Mike Hong and Lingjie Xu. Br100 gpgpu: Accelerating datacenter scale ai computing. In *2022 IEEE Hot Chips 34 Symposium (HCS)*, pages 1–22. IEEE Computer Society, 2022.
- [19] Chien-Chin Huang, Gu Jin, and Jinyang Li. Swapadvisor: Pushing deep learning beyond the gpu memory limit via smart swapping. In *Proceedings of the Twenty-Fifth International Conference on Architectural Support for Programming Languages and Operating Systems*, pages 1341–1355, 2020.
- [20] Qijing Huang, Aravind Kalaiah, Minwoo Kang, James Demmel, Grace Dinh, John Wawrzynek, Thomas Norell, and Yakun Sophia Shao. CoSA: Scheduling by Constrained Optimization for Spatial Accelerators. In *2021 ACM/IEEE 48th Annual International Symposium on Computer Architecture (ISCA)*, pages 554–566, Valencia, Spain, June 2021. IEEE.
- [21] Tian Jin and Seokin Hong. Split-cnn: Splitting window-based operations in convolutional neural networks for memory system optimization. In *Proceedings of the Twenty-Fourth International Conference on Architectural Support for Programming Languages and Operating Systems*, pages 835–847, 2019.
- [22] Jeff Johnson. Rethinking floating point for deep learning. *arXiv:1811.01721 [cs]*, November 2018. arXiv: 1811.01721.
- [23] Norman P. Jouppi, Doe Hyun Yoon, Matthew Ashcraft, Mark Gottscho, Thomas B. Jablin, George Kurian, James Laudon, Sheng Li, Peter Ma, Xiaoyu Ma, Thomas Norrie, Nishant Patil, Sushma Prasad, Cliff Young, Zongwei Zhou, and David Patterson. Ten Lessons From Three Generations Shaped Google's TPUv4i: Industrial Product. In *2021 ACM/IEEE 48th Annual International Symposium on Computer Architecture (ISCA)*, pages 1–14, Valencia, Spain, June 2021. IEEE.
- [24] Norman P Jouppi, Cliff Young, Nishant Patil, David Patterson, Gaurav Agrawal, Raminder Bajwa, Sarah Bates, Suresh Bhatia, Nan Boden, Al Borchers, et al. In-datacenter performance analysis of a tensor processing unit. In *Proceedings of the 44th annual international symposium on computer architecture*, pages 1–12, 2017.
- [25] Andrew Kerr, Duane Merrill, Julien Demouth, and John Tran. Cutlass: Fast linear algebra in cuda c++. *NVIDIA Developer Blog*, 2017.
- [26] Saif Khan and Alexander Mann. Ai chips: What they are and why they matter. table 3, page 24. cset.
- [27] Farzad Khorasani, Hodjat Asghari Esfeden, Nael Abu-Ghazaleh, and Vivek Sarkar. In-register parameter caching for dynamic neural nets with virtual persistent processor specialization. In *2018 51st Annual IEEE/ACM International Symposium on Microarchitecture (MICRO)*, pages 377–389. IEEE, 2018.
- [28] Benjamin Klenk, Nan Jiang, Greg Thorson, and Larry Dennison. An In-Network Architecture for Accelerating Shared-Memory Multiprocessor Collectives. In *2020 ACM/IEEE 47th Annual International Symposium on Computer Architecture (ISCA)*, pages 996–1009, Valencia, Spain, May 2020. IEEE.
- [29] Hyoungjun Kwon, Prasanth Chatarasi, Vivek Sarkar, Tushar Krishna, Michael Pellauer, and Angshuman Parashar. MAESTRO: A Data-Centric Approach to Understand Reuse, Performance, and Hardware Cost of DNN Mappings. *IEEE Micro*, 40(3):20–29, May 2020.
- [30] Youngeun Kwon and Minsoo Rhu. Beyond the memory wall: A case for memory-centric hpc system for deep learning. In *2018 51st Annual IEEE/ACM International Symposium on Microarchitecture (MICRO)*, pages 148–161. IEEE, 2018.
- [31] Yizhi Liu, Yao Wang, Ruofei Yu, Mu Li, Vin Sharma, and Yida Wang. Optimizing CNN model inference on CPUs. In *Proceedings of the 2019 USENIX Conference on Usenix Annual Technical Conference*, USENIX ATC '19, pages 1025–1040, Renton, WA, USA, July 2019. USENIX Association.
- [32] Graphcore Ltd. Graphcore: Accelerating machine learning for a world of intelligent machines.
- [33] Sparsh Mittal, Poonam Rajput, and Sreenivas Subramoney. A Survey of Deep Learning on CPUs: Opportunities and Co-Optimizations. *IEEE Transactions on Neural Networks and Learning Systems*, pages 1–21, 2021.
- [34] Anant V. Nori, Rahul Bera, Shankar Balachandran, Joydeep Rakshit, Om J. Omer, Avishai Abuhatzera, Belliappa Kuttanna, and Sreenivas Subramoney. Reduct: Keep it close, keep it cool! : Efficient scaling of dnn inference on multi-core cpus with near-cache compute. In *2021 ACM/IEEE 48th Annual International Symposium on Computer Architecture (ISCA)*, pages 167–180, 2021.
- [35] Tony Nowatzki, Vinay Gangadhar, Karthikeyan Sankaralingam, and Greg Wright. Pushing the limits of accelerator efficiency while retaining programmability. In *2016 IEEE International Symposium on High Performance Computer Architecture (HPCA)*, pages 27–39. IEEE, 2016.
- [36] NVIDIA. Nvidia tesla v100 gpu architecture. 2017.
- [37] Angshuman Parashar, Priyanka Raina, Yakun Sophia Shao, Yu-Hsin Chen, Victor A. Ying, Anurag Mukkara, Rangharajan Venkatesan, Bruce Khailany, Stephen W. Keckler, and Joel Emer. Timeloop: A Systematic Approach to DNN Accelerator Evaluation. In *2019 IEEE International Symposium on Performance Analysis of Systems and Software (ISPASS)*, pages 304–315, Madison, WI, USA, March 2019. IEEE.

- [38] Eric Qin, Ananda Samajdar, Hyoukjun Kwon, Vineet Nadella, Sudarshan Srinivasan, Dipankar Das, Bharat Kaul, and Tushar Krishna. SIGMA: A Sparse and Irregular GEMM Accelerator with Flexible Interconnects for DNN Training. In *2020 IEEE International Symposium on High Performance Computer Architecture (HPCA)*, pages 58–70, San Diego, CA, USA, February 2020. IEEE.
- [39] Vijay Janapa Reddi, Christine Cheng, David Kanter, Peter Mattson, Guenther Schmuelling, Carole-Jean Wu, Brian Anderson, Maximilien Breughe, Mark Charlebois, William Chou, Ramesh Chukka, Cody Coleman, Sam Davis, Pan Deng, Greg Diamos, Jared Duke, Dave Fick, J. Scott Gardner, Itay Hubara, Sachin Isgunji, Thomas B. Jablin, Jeff Jiao, Tom St. John, Pankaj Kanwar, David Lee, Jeffery Liao, Anton Likhomotov, Francisco Massa, Peng Meng, Paulius Micikevicius, Colin Osborne, Gennady Pekhimenko, Arun Tejusve Raghunath Rajan, Dilip Sequeira, Ashish Sirasao, Fei Sun, Hanlin Tang, Michael Thomson, Frank Wei, Ephrem Wu, Lingjie Xu, Koichi Yamada, Bing Yu, George Yuan, Aaron Zhong, Peizhao Zhang, and Yuchen Zhou. Mlperf inference benchmark. In *2020 ACM/IEEE 47th Annual International Symposium on Computer Architecture (ISCA)*, pages 446–459, 2020.
- [40] Albert Reuther, Peter Michaleas, Michael Jones, Vijay Gadepally, Siddharth Samsi, and Jeremy Kepner. Survey of Machine Learning Accelerators. In *2020 IEEE High Performance Extreme Computing Conference (HPEC)*, pages 1–12, Waltham, MA, USA, September 2020. IEEE.
- [41] Karthikeyan Sankaralingam, Tony Nowatzki, Vinay Gangadhar, Preyas Shah, Michael Davies, William Galliher, Ziliang Guo, Jitu Khare, Deepak Vijay, Poly Palamuttam, Maghawan Punde, Alex Tan, Vijay Thiruvengadam, Rongyi Wang, and Shunmiao Xu. The Mozart reuse exposed dataflow processor for AI and beyond: industrial product. In *Proceedings of the 49th Annual International Symposium on Computer Architecture*, pages 978–992, New York New York, June 2022. ACM.
- [42] Yakun Sophia Shao, Jason Clemons, Rangharajan Venkatesan, Brian Zimmer, Matthew Fojtik, Nan Jiang, Ben Keller, Alicia Klinefelter, Nathaniel Pinckney, Priyanka Raina, Stephen G. Tell, Yanqing Zhang, William J. Dally, Joel Emer, C. Thomas Gray, Bruce Khailany, and Stephen W. Keckler. Simba: Scaling Deep-Learning Inference with Multi-Chip-Module-Based Architecture. In *Proceedings of the 52nd Annual IEEE/ACM International Symposium on Microarchitecture*, pages 14–27, Columbus OH USA, October 2019. ACM.
- [43] Muthian Sivathanu, Tapan Chugh, Sanjay S Singapuram, and Lidong Zhou. Astra: Exploiting predictability to optimize deep learning. In *Proceedings of the Twenty-Fourth International Conference on Architectural Support for Programming Languages and Operating Systems*, pages 909–923, 2019.
- [44] Linghao Song, Fan Chen, Youwei Zhuo, Xuehai Qian, Hai Li, and Yiran Chen. Accpar: Tensor partitioning for heterogeneous deep learning accelerators. In *2020 IEEE International Symposium on High Performance Computer Architecture (HPCA)*, pages 342–355. IEEE, 2020.
- [45] Aaron Stillmaker and Bevan Baas. Scaling equations for the accurate prediction of CMOS device performance from 180 nm to 7 nm. *Integration*, 58:74–81, June 2017.
- [46] Dana Vantrease, Robert Schreiber, Matteo Monchiero, Moray McLaren, Norman P Jouppi, Marco Fiorentino, Al Davis, Nathan Binkert, Raymond G Beausoleil, and Jung Ho Ahn. Corona: System implications of emerging nanophotonic technology. *ACM SIGARCH Computer Architecture News*, 36(3):153–164, 2008.
- [47] Rangharajan Venkatesan, Priyanka Raina, Yanqing Zhang, Brian Zimmer, William J. Dally, Joel Emer, Stephen W. Keckler, Bruce Khailany, Yakun Sophia Shao, Miaorong Wang, Jason Clemons, Steve Dai, Matthew Fojtik, Ben Keller, Alicia Klinefelter, and Nathaniel Pinckney. MAGNet: A Modular Accelerator Generator for Neural Networks. In *2019 IEEE/ACM International Conference on Computer-Aided Design (ICCAD)*, pages 1–8, Westminster, CO, USA, November 2019. IEEE.
- [48] Snehlil Verma, Qinzhe Wu, Bagus Hanindhito, Gunjan Jha, Eugene B. John, Ramesh Radhakrishnan, and Lizy K. John. Demystifying the mlperf training benchmark suite. In *2020 IEEE International Symposium on Performance Analysis of Systems and Software (ISPASS)*, pages 24–33, 2020.
- [49] Bob Wheeler. Sambanova takes on nvidia’s dgx. Feb 2021.
- [50] Yannan Nellie Wu, Joel S. Emer, and Vivienne Sze. Accelergy: An Architecture-Level Energy Estimation Methodology for Accelerator Designs. In *2019 IEEE/ACM International Conference on Computer-Aided Design (ICCAD)*, pages 1–8, Westminster, CO, USA, November 2019. IEEE.
- [51] Xilinx. Versal: The first adaptive compute acceleration platform. 2020.
- [52] Hao Zhang et al. *Flexible Multiple-Precision Fused Arithmetic Units for Efficient Deep Learning Computation*. PhD thesis, University of Saskatchewan, 2019.
- [53] Size Zheng, Renze Chen, Anjiang Wei, Yicheng Jin, Qin Han, Liqiang Lu, Bingyang Wu, Xiuhong Li, Shengen Yan, and Yun Liang. Amos: enabling automatic mapping for tensor computations on spatial accelerators with hardware abstraction. In *ISCA*, pages 874–887, 2022.